

Actin and Myosin Function in Acanthamoeba

T. D. Pollard, U. Aebi, J. A. Cooper, W. E. Fowler, D. P. Kiehart, P. R. Smith and P. C. Tseng

Phil. Trans. R. Soc. Lond. B 1982 **299**, 237-245

doi: 10.1098/rstb.1982.0129

Email alerting service

Receive free email alerts when new articles cite this article - sign up in the box at the top right-hand corner of the article or click [here](#)

To subscribe to *Phil. Trans. R. Soc. Lond. B* go to: <http://rstb.royalsocietypublishing.org/subscriptions>

Actin and myosin function in *Acanthamoeba*

BY T. D. POLLARD, U. AEBI, J. A. COOPER, W. E. FOWLER,
D. P. KIEHART, P. R. SMITH AND P. C. TSENG

*Department of Cell Biology and Anatomy, Johns Hopkins University Medical School,
Baltimore, Maryland 21205, U.S.A.*

[Plates 1 and 2]

We have studied the functions of contractile proteins in *Acanthamoeba* by a combination of structural, biochemical and physiological approaches. We used electron microscopy and image processing to determine the three-dimensional structure of actin and the orientation of the molecule in the actin filament. We measured the rate constants for actin filament elongation and re-evaluated the effect of $MgCl_2$ on the filament nucleation process. In *Acanthamoeba* actin polymerization is regulated, at least in part, by profilin, which binds to actin monomers, and by capping protein, which both nucleates polymerization and blocks monomer addition at the 'barbed' end of the filament. To test for physiological functions of myosin-II, we produced a monoclonal antibody that inhibits the actin-activated ATPase. When microinjected into living cells, this active-site-specific antibody inhibits amoeboid locomotion. We expect that similar experiments can be used to test for the physiological functions of the other components of the *Acanthamoeba* contractile system.

INTRODUCTION

Single cells have the capacity for a variety of distinctive movements including cytokinesis, organelle movements, cytoplasmic streaming, amoeboid movement, and extension and retraction of filopodia and other surface processes. The mechanisms of these movements are thought to involve complex interactions between actin, myosin and a myriad of accessory proteins, which acting in concert impart structure, produce force and maintain control during contractile events.

In our view, the best way to approach the complex questions regarding mechanisms of cell motility is to isolate and characterize the molecules composing the motile machinery, to locate each protein in the cell and to devise ways of testing directly for the function of each in the living cell. *Acanthamoeba castellanii* is a favourable organism for such studies because (i) it can be grown inexpensively in kilogram quantities to provide material for biochemical studies, (ii) its phagocytosis (Weisman & Korn 1967) and pinocytosis (Bowers & Olszewski 1972) are well characterized, (iii) it is activity motile, (iv) its proteins are highly antigenic in rabbits and mice, and (v) it can be microinjected into for physiological experiments. Work in our laboratory and in E. D. Korn's laboratory at the National Institutes of Health has identified 14 different proteins that are likely to participate in motile force generation (table 1).

In this paper we present some of our recent results on the structure and function of actin and myosin in *Acanthamoeba*. Our most important progress has been on the three-dimensional structure of actin, on the mechanism of actin polymerization and the regulation of actin polymerization by binding proteins. We also describe our recent experiments with monoclonal

[91]

TABLE 1. *ACANTHAMOEBA* CONTRACTILE PROTEINS

| protein | selected references |
|------------------|--|
| actin | Pollard <i>et al.</i> (1970), Weihing & Korn (1971), Gordon <i>et al.</i> (1977) |
| profilin | Reichstein & Korn (1979), Mockrin & Korn (1980), Tseng & Pollard (1982), Tobacmann & Korn (1982) |
| capping protein | Isenberg <i>et al.</i> (1980) |
| gelactin-23k | Maruta & Korn (1977a) |
| gelactin-28k | Maruta & Korn (1977a) |
| gelactin-33k | Maruta & Korn (1977a), MacLean-Fletcher & Pollard (1980) |
| gelactin-38k | Maruta & Korn (1977a), MacLean-Fletcher & Pollard (1980) |
| gelation protein | Pollard (1981) |
| myosin-IA | Pollard & Korn (1973a), Maruta <i>et al.</i> (1979) |
| myosin-IB | Maruta <i>et al.</i> (1979) |
| myosin-IC | Maruta <i>et al.</i> (1979) |
| myosin-I kinase | Pollard & Korn (1973b), Maruta & Korn (1977c) |
| myosin-II | Maruta & Korn (1977b), Pollard <i>et al.</i> (1978) |
| myosin-II kinase | Collins & Korn (1980), Côté <i>et al.</i> (1981) |

antibody microinjection, which show great promise as an approach to examine the function of myosin isozymes inside living cells.

ACTIN STRUCTURE

Knowledge about the three-dimensional structure and conformation of actin is fundamental to an eventual understanding of its function at the molecular level. We have obtained two- and three-dimensional information about the actin molecule by image processing of electron micrographs recorded from negatively stained, highly ordered, two-dimensional crystalline sheets of *Acanthamoeba* actin (figure 1a, plate 1) (Aebi *et al.* 1980, 1981). When viewed in projection normal to the sheet plane, the molecule appears elongated ($56\text{Å} \times 33\text{Å}^\dagger$) and distinctly bilobed,

$$\dagger 1 \text{ Å} = 10^{-10} \text{ m} = 10^{-1} \text{ nm.}$$

DESCRIPTION OF PLATE 1

FIGURE 1. (a) Tilt pair (0° and 60°) of a negatively stained (7.5 mg ml^{-1} uranyl formate) 'rectangular' crystalline actin sheet consisting of two single-layered 'basic' sheets associated back-to-back and staggered by half a unit cell perpendicular to the longer axis of the sheet; the tilted view was recorded first under minimum dose conditions (less than $10 \text{ e}^-/\text{Å}^2$). Bar = $1 \mu\text{m}$.

(b) Single-sided computer filtration of an untilted rectangular sheet; the filtered image reveals the packing of the actin molecules in projection in the basic sheet, which is one actin molecule thick and includes two actin molecules in its near-rectangular unit cell ($a = 56 \text{ Å}$, $b = 65 \text{ Å}$, $\gamma = 86^\circ$) related to each other by a twofold axis of symmetry normal to the sheet plane. Averaging was extended over more than 2000 unit cells. Protein is represented as light and the negative stain as dark; the two black contours include 25 and 65% of the mass of the actin molecule, respectively.

(c) Balsa-wood model of 2×2 actin molecules as revealed in the basic sheet upon three-dimensional reconstruction from a set of tilted views of rectangular sheets as shown in (a); the contouring level of the 15 Å resolution three-dimensional model has been chosen to include 65% of the mass of the actin molecule.

(d) Model of a 'synthetic' actin filament built from actin molecules as obtained from the map shown in (c) and using a contouring level to include 60% of the mass of the actin molecule. The model has the proper helical symmetry and stagger between the two helical strands. The angular orientation of the actin molecule relative to the filament axis was chosen so as (i) to optimize the contact area between the two strands and (ii) to get an optimal fit between the model and the three-dimensional model of the actin filament shown in (e) obtained by three-dimensional reconstruction from actin filament paracrystals as shown in (f). Bar = 50 Å .

(e) Model of an actin filament stretch reconstructed from actin filament paracrystals; the contouring level has been chosen to include 60% of the mass of the actin molecule. Bar = 50 Å .

(f) Electron micrographs of negatively stained (7.5 mg ml^{-1} uranyl formate) actin filaments and polylysine-induced actin filament paracrystals. Bars = $1 \mu\text{m}$. (Work of U. Aebi, W. E. Fowler & P. R. Smith.)

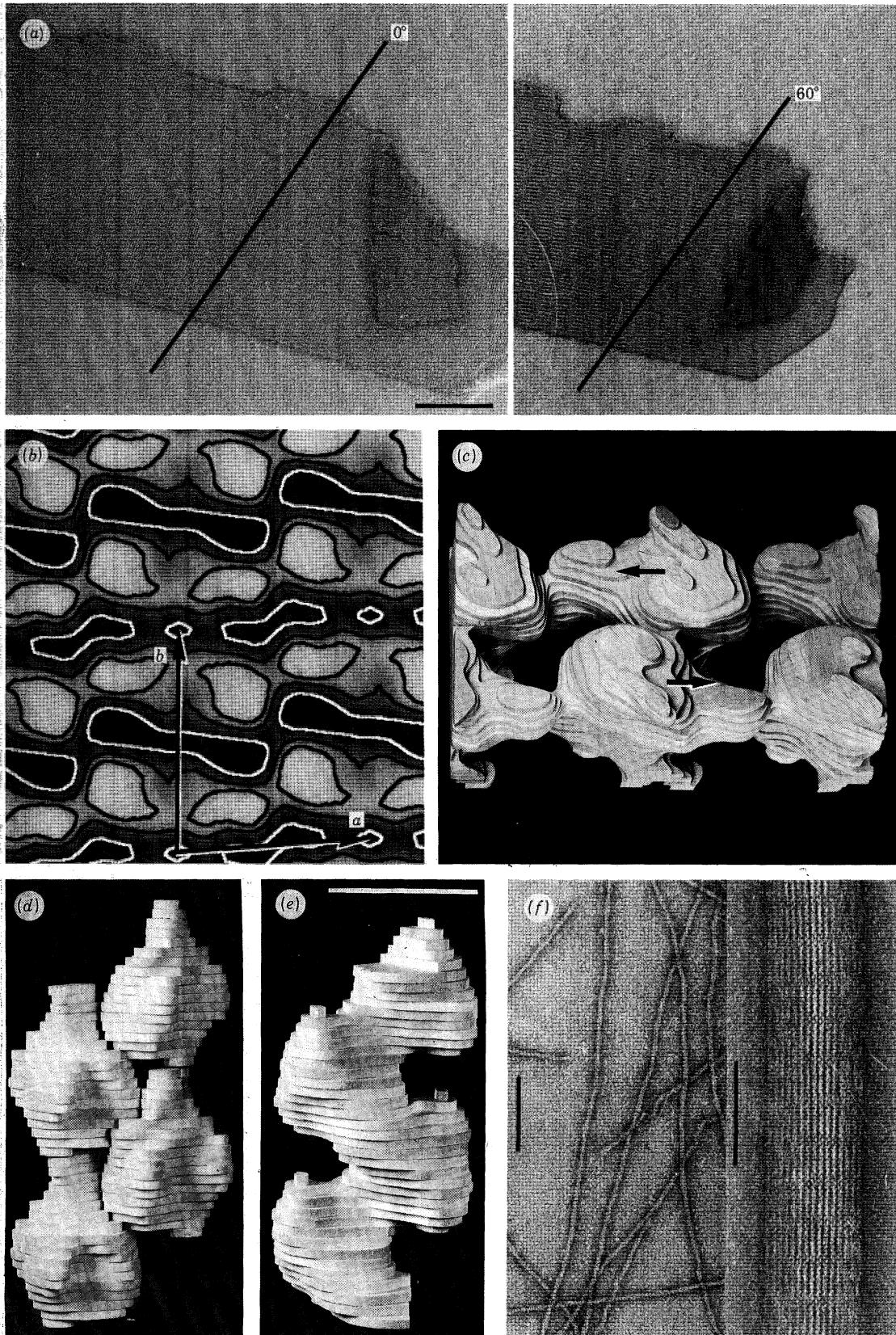


FIGURE 1. For description see opposite.

(Facing p. 238)

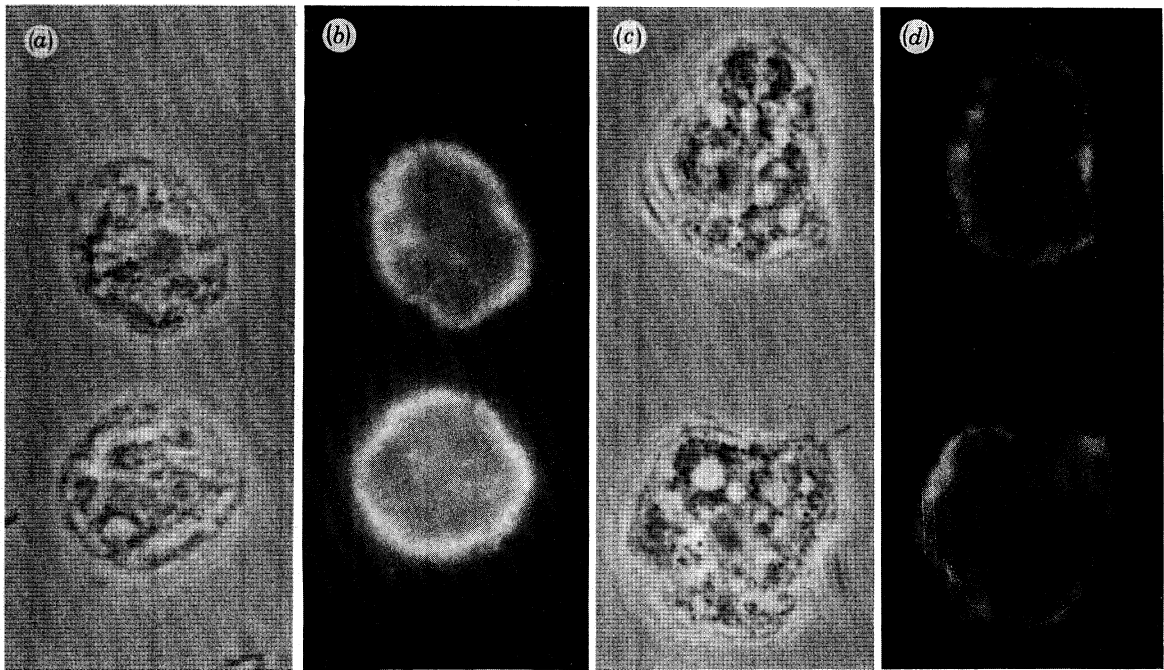


FIGURE 4. Localization in *Acanthamoeba* of actin filaments as shown with NBD-phalloidin (*a*, *b*) and capping protein with a purified antibody (*c*, *d*). Phase contrast (*a*, *c*) and fluorescence (*b*, *d*) micrographs of whole cells fixed with formaldehyde and permeabilized with acetone. (Work of J. A. Cooper.)

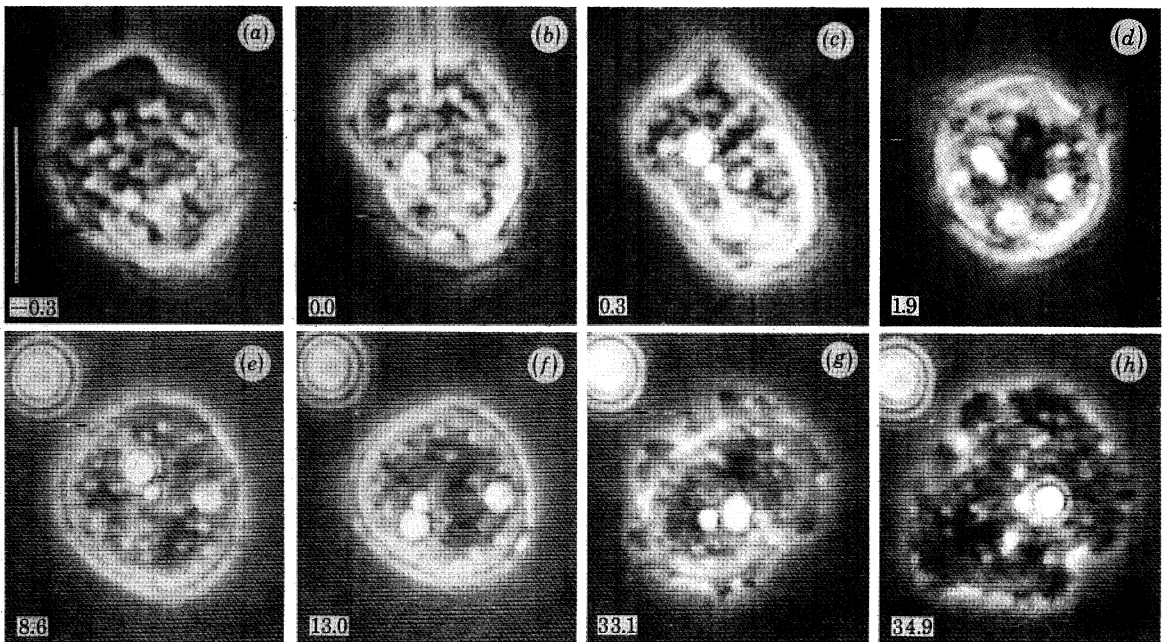


FIGURE 5. Microinjection of a living *Acanthamoeba* with 14 mg ml^{-1} monoclonal antibody MII.1 against myosin-II. This is a time sequence of phase contrast micrographs taken from (*a*) 0.3 min before microinjection to (*h*) 34.9 min afterwards. A droplet of oil equivalent in volume to the antibody injection ($2.6 \text{ pl} = 3.5\%$ of cell volume) is shown to the upper left of the cell in (*e*)–(*h*).

with a 'major' and 'minor' lobe separated by a 'cleft' (figure 1*b*) (Aebi *et al.* 1981). By tilting the specimen in the electron microscope up to $\pm 60^\circ$ (figure 1*a*), we have collected data that allowed us to compute a 15 Å resolution three-dimensional model of the actin molecule. This model reveals the overall size, shape and major surface topography of the actin molecule (figure 1*c*). In this model, actin has overall dimensions of 56 Å × 33 Å × 43 Å and is roughly the shape of a 'lumpy pear'. One end is considerably more massive than the other. Owing to the use of negative stain, however, neither the two- nor the three-dimensional models have revealed any 'internal' features (e.g. secondary structure) of the molecule. These details will eventually be filled in by X-ray diffraction work in progress on actin co-crystals with DNase I (Suck *et al.* 1981) or profilin (Carlsson *et al.* 1976), or perhaps by further electron microscopic analysis of unstained crystalline actin sheets (Fowler & Aebi, unpublished).

Since the biologically important supramolecular assembly of actin in muscle and non-muscle cells is the actin filament, we have attempted to build a 'synthetic' filament from the three-dimensional model of actin determined from the crystalline sheets (figure 1*d*). To have a reference structure for the filament, we computed a preliminary 30 Å resolution model (figure 1*e*) from negatively stained actin paracrystals (figure 1*f*). These paracrystals were induced by polylysine and some are ordered enough to diffract to about 25 Å resolution (Fowler & Aebi 1982). The most striking common features of both the native and synthetic filaments are the strong lateral and weak longitudinal contacts of the actin molecules within the filament. This weak 'intra-strand connectivity' has actually been reported previously from image reconstructions of thin-filament paracrystals (Wakabayashi *et al.* 1975). Our model-building experiments were greatly facilitated by the apparent presence of naturally occurring lateral 'complementary surfaces' found on the model of the actin molecules, which 'forced' it into the proper helical symmetry required by the filament after aligning the 56 Å axis of the molecule with the filament axis and staggering the molecules in the two strands by 56 Å/2 with respect to each other (figure 1*d*). The weak longitudinal contacts give rise, of course, to the alternating 'sawtooth and smooth' appearance of negatively stained filaments viewed in projection (figure 1*f*). One of our next goals will be to identify the 'barbed' and 'pointed' ends of the filament on the model of the actin molecule, because this should then enable us to identify the sites on the surface of the actin molecule that bind tropomyosin and myosin.

ACTIN POLYMERIZATION

During polymerization actin monomers must undergo a series of association reactions, forming first a dimer and then higher-order polymers (figure 2). Since the classic work of Oosawa and his colleagues over the past 20 years (reviewed in Oosawa & Asakura 1975), it has been recognized that elongation is rapid and that a slow early step (or steps) accounts for the sigmoidal time course of polymerization of bulk samples. Kasai *et al.* (1962) found that the initial rate of polymerization increases with the third to fourth power of the actin concentration and concluded that the formation of nuclei consisting of three or four actin molecules is the rate-limiting step. Later it was learned that actin monomers undergo a conformational change under polymerizing conditions (Rich & Estes 1976; Rouayrenc & Travers 1981). This may be an activated (A_1^*) form of the monomer and an intermediate in the polymerization pathway, but has not as yet been proved.

Remarkably, little was learned before 1980 about rate constants for the individual steps in

the polymerization of actin. The problem is that it is difficult or impossible to measure the rates of individual reactions in bulk samples where the activation, nucleation and elongation steps occur simultaneously.

Because a complete understanding of the mechanism of actin polymerization will depend on a knowledge of all of the rate constants in figure 2 (plus the rates of any other reactions along this pathway), we have started to measure these essential constants. To date we have measured the rate constants for monomer association and dissociation at the two ends of the filament

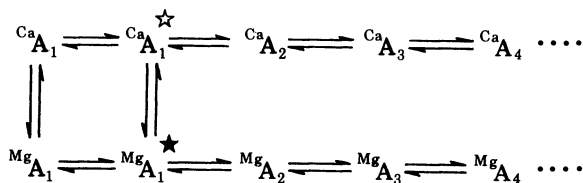


FIGURE 2. Possible early steps in actin polymerization. 'A' is actin. The subscripts indicate state of aggregation. The superscripts 'Ca' and 'Mg' indicate bound Ca^{2+} or Mg^{2+} . The superscript star represents an unspecified activation step induced by polymerizing concentrations of salt.

TABLE 2. ACTIN ELONGATION RATE CONSTANTS

| solution conditions | association constant $\mu\text{M}^{-1} \text{s}^{-1}$ | | dissociation constant s^{-1} | | reference |
|---|--|---------|--|---------|-----------|
| | barbed | pointed | barbed | pointed | |
| 20 mM KCl, 0.04 mM CaCl_2 , pH 7 | 5.9 | 0.8 | 6.0 | 0.7 | 1 |
| 100 mM KCl, 0.2 mM CaCl_2 , pH 7 | 9.5 | 1.1 | 4.2 | 0.8 | 3 |
| 100 mM KCl, 1 mM MgCl_2 , 0.2 mM CaCl_2 , pH 7 | 10.2 | — | 7.0 | — | 3 |
| 100 mM KCl, 1 mM MgCl_2 , 0.2 μM CaCl_2 , pH 7 | 6.9 | 1.1 | -3.3 | -0.4 | 3 |
| 75 mM KCl, 5 mM MgSO_4 , 0.04 mM CaCl_2 , pH 7 | 8.8 | 2.2 | 2.0 | 1.4 | 1 |
| 75 mM KCl, 5 mM MgCl_2 , pH 7.3 | 10 | 1.5 | 1.5 | 0.5 | 2 |

References: 1, Pollard & Mooseker (1981); 2, Bonder & Mooseker (1981); 3, Cooper *et al.* (1982).

under a variety of conditions (table 2) (Pollard & Mooseker 1981; Cooper *et al.* 1982) and have investigated how the slow phase of polymerization depends on actin monomer concentration in the presence of Ca^{2+} or Mg^{2+} (Cooper *et al.* 1982).

We began our analysis with the elongation reaction, because it is more accessible than the earlier steps. Our approach has been to use electron microscopy to measure the absolute rate of growth of filaments from the ends of morphologically identifiable nuclei as a function of the actin monomer concentration. We have used as nuclei microvillar actin filament bundles (Pollard & Mooseker 1981) or myosin subfragment-1 decorated actin filaments stabilized by glutaraldehyde cross-linking (Cooper *et al.* 1982). Bonder & Mooseker (1981) made similar measurements by using the bundle of actin filaments from *Limulus* sperm as nuclei. The results with the three types of nuclei are the same (table 2). This method has some limitations, including a delay in the onset of growth of some of the filaments, some filament breakage and the large amount of work required to collect the data, but it is currently the only way to measure absolute elongation rates. Because of the limitations the measured rates are likely to be somewhat less than the actual rates.

The association rate constant at the barbed end is very large ($10^7 \text{ M}^{-1} \text{ s}^{-1}$) and independent (within the limits of experimental error) of the solution conditions that have been tested (table

2). This suggests that this reaction is diffusion-limited. The association rate constant at the pointed end is one-fifth to one tenth of this, but at $10^6 \text{ M}^{-1} \text{ s}^{-1}$ it is among the largest rate constants measured for protein associations. It, too, is relatively insensitive to solution conditions. The dissociation rate constants are small and more difficult to measure accurately, but are also approximately the same in various buffers.

Beyond these rate constants and the critical concentration for polymerization, little is known about the elongation reaction. We do not know with certainty what aspect of monomer association is rate-limiting. At the barbed end the rate-limiting step is probably the formation of the collision intermediate, but it could be a subsequent step such as the conformational change in the actin molecule that gives rise to an absorbance change in the ultraviolet (Higashi & Oosawa 1965). At the pointed end the rate-limiting step could even be ATP hydrolysis, a reaction that lags behind polymerization in bulk samples (Pardee & Spudich 1982).

The early steps in actin polymerization are much more difficult to study, because they cannot be measured directly with currently available assays. We have extended the original approach of Kasai *et al.* (1960) to examine the early steps indirectly by measuring the dependence of the slow phase of polymerization on the actin monomer concentration. We confirmed that plots of log (initial rate of viscosity change) against log (actin concentration) are linear with slopes in the range of 2.5–4.5 under several conditions. The slope of such a plot gives the order of the reaction. We found that it is very difficult to obtain the initial rates by extrapolating the viscosity plots back to zero time. Furthermore, the shear during viscosity measurements accelerates polymerization, raising additional questions about the validity of these initial rate measurements. Consequently, we turned to a fluorimetric assay for polymerization by using actin labelled with pyrene at Cys 373 (Kouyama & Mihashi 1981). We used the inverse delay time as the measure for the slow phase. Plots of log (inverse delay time) against log (actin concentration) are linear and the slopes approach unity in the presence of Mg^{2+} and are about 2 in the presence of Ca^{2+} . The most straightforward interpretation of these findings is that nucleation is the rate-limiting step when Ca^{2+} is bound to the high-affinity divalent cation binding site. A dimer is presumably the nucleus for rapid elongation, and thus nucleation is the rate-limiting step under these circumstances. In contrast, nucleation may not be the rate-limiting step in the presence of Mg^{2+} , because the rate of the slow phase is first-order in actin. One interpretation is that the formation of nuclei by Mg^{2+} -actin is faster than by Ca^{2+} -actin and also faster than some preceding step, which is therefore rate limiting. What could this first-order rate-limiting step be? We know of only two steps that might occur before subunit association. One is a conformational change induced in monomers by KCl, which was first detected by resistance to proteolysis (Rich & Estes 1976) and later by an absorption change in the ultraviolet (Rouayrenc & Travers 1981). The other reaction is the exchange of bound Mg^{2+} for Ca^{2+} (Frieden 1982) that occurs when we add the polymerizing buffer containing 100 mM KCl and 1 mM MgCl_2 to the actin, which has been prepared in CaCl_2 . There may also be currently unrecognized steps. Additional work will be required to distinguish between these possibilities.

REGULATION OF ACTIN POLYMERIZATION

The regulation of actin polymerization must present a major challenge for a cell like *Acanthamoeba*, which contains a high concentration (250 μM) of actin. Under physiological conditions virtually all of this actin would polymerize spontaneously and permanently into filaments.

[95]

Although the story is far from complete, we now recognize that *Acanthamoeba* and other cells can regulate their actin polymerization in three different ways: sequestration of actin monomers in a non-polymerizable complex, capping of the ends of actin filaments, and cross-linking actin filaments (Craig & Pollard 1982) (figure 3).

Profilin is a monomer-sequestering protein in *Acanthamoeba*. It was first purified by Reichstein & Korn (1979), who showed that it prolonged the lag phase at the outset of *Acanthamoeba* actin polymerization. Mockrin & Korn (1980) also showed that it promoted the exchange of the nucleotide bound to actin. We have extended the analysis of how profilin modifies actin polymerization (Tseng & Pollard 1982). Tobacmann & Korn (1982) have carried out similar

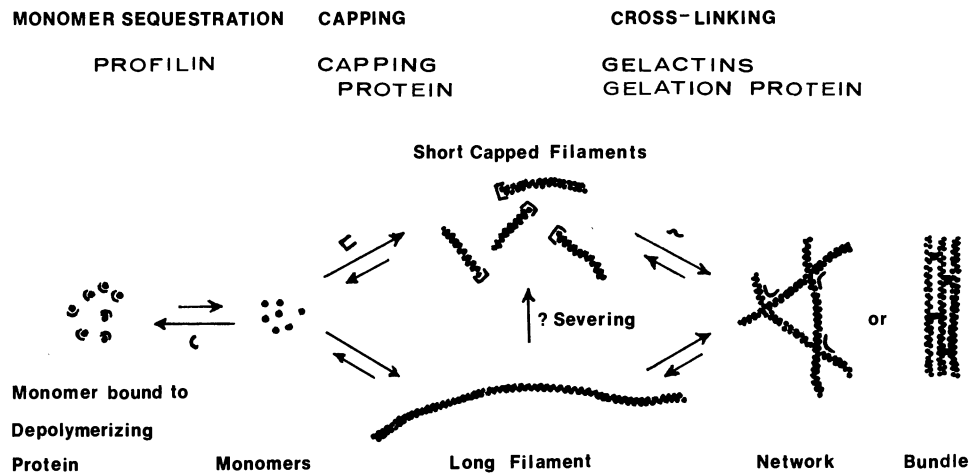


FIGURE 3. Three classes of actin-binding proteins in *Acanthamoeba*. (Modified from Craig & Pollard (1982).)

experiments. In most respects the interaction of *Acanthamoeba* profilin with actin is very straightforward. In 50 mM KCl it binds to *Acanthamoeba* G-actin with moderately high affinity ($K_d = 1-4 \mu\text{M}$), and the actin in the complex is not available for polymerization. Consequently, low concentrations of profilin reduce the rate and extent of polymerization in 50 mM KCl. When profilin is added to polymerized actin, a new equilibrium is slowly attained, with the final extent of polymerization determined by the concentration of the two proteins. These effects are all explained by mass action. The effect of amoeba profilin on muscle actin polymerization can be explained in the same way, except that the affinity of the amoeba profilin for muscle actin is lower by an order of magnitude.

Mg^{2+} has a pronounced effect on the interaction of *Acanthamoeba* profilin with either amoeba or muscle actin. Although profilin prolongs the lag phase of polymerization for both actins in 1 mM MgCl_2 , 50 mM KCl, it has no effect on the rate of elongation (measured by electron microscopy) or the steady-state extent of polymerization. Thus, *Acanthamoeba* profilin appears to bind only weakly to G-actin in Mg^{2+} . Only low concentrations of Mg^{2+} are required for this effect. The half-maximal effect occurs at Mg^{2+} concentrations of about 30–40 μM , so that magnesium may be binding to the high-affinity site on actin. The mechanism by which profilin prolongs the lag phase under conditions where it does not appear to bind to monomers at steady state has not been established, but we speculate that profilin might bind to actin monomers and inhibit the rate of their activation.

These properties of profilin suggest that profilin may be an actin monomer buffer in the cell.

Further information about the concentrations of actin, profilin and Mg^{2+} will be necessary to substantiate this conclusion and to calculate the free actin monomer concentration *in vivo*.

The second actin regulatory protein is capping protein (Isenberg *et al.* 1980). This protein blocks monomer addition at the barbed ends of growing actin filaments but can also nucleate actin polymerization. The capping and nucleating activities do not depend on Ca^{2+} . Capping protein consists of a heterodimer of immunologically distinct polypeptides with molecular masses of 28 and 31 kDa (Cooper *et al.* 1981). The sedimentation coefficient (4.8 *S*) and Stokes radius (3.8 nm) suggest that it is slightly asymmetric. The capping protein is localized primarily in the cortex of the cell, along with most of the polymerized actin (figure 4, plate 2).

There is no direct evidence about the functions of capping protein in the amoeba, but the established properties of the protein have led to some speculation about its functions. There is probably enough capping protein in *Acanthamoeba* to cap all of the filaments in the cell. Provided that the affinity is high enough, this would prevent end-to-end annealing and subunit exchange at the barbed end of the amoeba's actin filaments. This feature, and its nucleating activity, suggest that capping protein is one factor that together with profilin determines the number and length of the filaments in the cell. If any cellular structures have affinity for capping protein, these structures would then become potential sites for actin filament anchorage or nucleation.

MONOCLONAL ANTIBODY MICROINJECTION: A TEST FOR FUNCTION IN THE LIVING CELL

The identification, purification and characterization of new contractile proteins from *Acanthamoeba* or other cells leads to speculation about their precise physiological function in living cells. In the absence of specific drugs that can inhibit the function of each of these proteins *in vivo*, and given that genetic manipulation of *Acanthamoeba* through the analysis of motility mutants has not been possible, we have embarked on microinjection studies, with antibodies as inhibitors of contractile protein function *in vivo*.

We produced more than 100 mouse lymphocyte hybridomas secreting antibodies to *Acanthamoeba* myosin-I or myosin-II (Kiehart *et al.* 1982). So far 22 cell lines producing monoclonal anti-myosin-II have been cloned and grown as Ascites tumours to produce sufficient quantities of antibody for purification and detailed characterization. In addition, eight different monoclonal antibodies to myosin-I have been obtained in large quantities. All of the antimyosin-II monoclonal antibodies react exclusively with the myosin-II heavy chain among the *Acanthamoeba* proteins. The antimyosin-I monoclonals react with the myosin-I heavy chain and about half also react with myosin-II heavy chain. This demonstrates that these otherwise very different myosins share a few common sequences. Most of the antimyosin-II antibodies react with the 105 kDa proteolytic fragment of the myosin-II heavy chain that comprises the entire tail and one-third of the head of the molecule (Collins *et al.* 1982). Two of 22 react with the 70 kDa peptide that makes up the remaining two-thirds of the head. Competitive binding assays indicate that most of the antibodies bind to different sites on the myosin, although there are several sites where two to four different antibodies bind. A preliminary electron microscopic study to discover the locations of the binding sites of two of the antibodies that react with the 105 kDa peptide revealed that one (MII.1) binds to the heads and the other (MII.3) binds to the end of the tail. Some, but not all, of these monoclonal antibodies inhibit the actin-activated Mg^{2+} ATPase of myosin-II. MII.1 is one of the inhibitory antibodies. None of 15 antibodies

tested inhibits the myosin-II Ca^{2+} ATPase in the absence of actin. Those antibodies that bind to the tail, such as MII.3, appear to be capable of blocking assembly of myosin-II into filaments.

The availability of large quantities of these active-site-specific monoclonal antibodies to myosin-II makes it possible to begin testing myosin-II functions in living cells. We have injected high concentrations of antibody MII.1 in a low ionic strength sucrose buffer into *Acanthamoeba* (figure 5, plate 2). Preliminary experiments indicate that within 5–10 min the cells round up and stop locomoting. In addition, the surface movements of the cell, including extension and retraction of filopodia and spreading of lamellopodia, also stop. Remarkably, the saltatory movements of organelles in the endoplasm and contraction of the contractile vacuole continue unabated. After a period of time (30–90 min) the injected cells recover completely and resume normal locomotion. We have followed the fate of injected antibody MII.1 labelled with rhodamine. Initially the antibody is distributed uniformly throughout the cytoplasm, but by the time that the cell starts to recover, the fluorescence becomes localized in discrete foci that we presume to be digestive vacuoles. Thus the cell seems to be capable of removing this noxious antibody from its cytoplasm by autophagy, explaining how it recovers its ability to move. This feature demonstrates the reversibility of the antibody treatment. Control injections of buffer alone or a monoclonal antibody to muscle myosin, which does not react with *Acanthamoeba* myosin, do not inhibit cell movements.

Our interpretation of these initial experiments is that myosin-II is required for amoeboid movement and the surface activity of the cell, but not for saltatory organelle movements. This must be confirmed by further experiments with other antibodies that inactivate myosin-II activity by binding to different sites. It will, of course, also be of great interest to determine whether these antibodies alter other motile processes in the cell, including pinocytosis, phagocytosis, cytokinesis and mitosis, and which, if any, movements require myosin-I. If any movements are unaffected by antibodies to both myosins, one would have presumptive evidence for the existence of a new mechanochemical system in the cell.

We expect that this approach will allow us to test in some detail which cellular activities depend on each of the *Acanthamoeba* myosins. An unexpected benefit may be the opportunity to test for the function of different parts of the myosin molecules by injecting antibodies that bind to the various parts of the molecule. For example, those antibodies that bind to the tail and inhibit polymerization into bipolar filaments can be used to test whether filaments are required for movement.

Finally, it is obvious that similar antibody microinjection experiments can be carried out for each of the components of the cell's contractile apparatus. The key to interpreting these experiments will be, just as with myosin, a thorough characterization of the interaction of each new monoclonal antibody with its purified antigen.

This work was supported by N.I.H. Research Grants nos GM-26132, GM-26338, GM-27765 and GM-26723, Muscular Dystrophy Association Research Grants and Postdoctoral Fellowships and N.I.H. Medical Scientist Training Program no. GM-7309.

REFERENCES

- Aebi, U., Fowler, W. E., Isenberg, G., Pollard, T. D. & Smith, P. R. 1981 *J. Cell Biol.* **91**, 340–351.
 Aebi, U., Smith, P. R., Isenberg, G. & Pollard, T. D. 1980 *Nature, Lond.* **288**, 296–298.
 Bonder, E. M. & Mooseker, M. S. 1981 *J. Cell Biol.* **91**, 306a.

- Bowers, B. & Olszewski, T. E. 1972 *J. Cell Biol.* **53**, 681–694.
- Carlsson, L., Nystrom, L.-E., Lindberg, U., Kannan, K. K., Cid-Dresdner, H. & Lovgren, S. 1976 *J. molec. Biol.* **105**, 353–366.
- Collins, J. H., Côté, G. P. & Korn, E. D. 1982 *J. biol. Chem.* **257**, 4529–4534.
- Collins, J. H. & Korn, E. D. 1980 *J. biol. Chem.* **255**, 8011–8014.
- Cooper, J. A., Isenberg, G. & Pollard, T. D. 1981 *J. Cell Biol.* **91**, 299a.
- Cooper, J. A., Tseng, T. Y. & Pollard, T. D. 1982 *Biophys. J.* **37**, 191a.
- Côté, G. P., Collins, J. H. & Korn, E. D. 1981 *J. biol. Chem.* **256**, 12811–12816.
- Craig, S. W. & Pollard, T. D. 1982 *Trends biochem. Sci.* **7**, 88–92.
- Fowler, W. E. & Aebi, U. A. 1982 *J. Cell Biol.* **93**, 452–458.
- Frieden, C. 1982 *J. biol. Chem.* **257**, 2882–2886.
- Gordon, D. S., Boyer, J. L. & Korn, E. D. 1977 *J. biol. Chem.* **252**, 8300–8309.
- Higashi, S. & Oosawa, F. 1965 *J. molec. Biol.* **12**, 843–865.
- Isenberg, G., Aebi, U. & Pollard, T. D. 1980 *Nature, Lond.* **288**, 455–459.
- Kasai, M., Askura, S. & Oosawa, F. 1962 *Biochim. biophys. Acta* **57**, 22–30.
- Kiehart, D. P., Kaiser, D. A. & Pollard, T. D. 1982 *Biophys. J.* **37**, 40.
- Kouyama, T. & Mihashi, K. 1981 *Eur. J. Biochem.* **114**, 33–38.
- MacLean-Fletcher, S. & Pollard, T. D. 1980 *J. Cell Biol.* **85**, 414–428.
- Maruta, H., Gadasi, H., Collins, J. H. & Korn, E. D. 1979 *J. biol. Chem.* **254**, 3624–3630.
- Maruta, H. & Korn, E. D. 1977a *J. biol. Chem.* **252**, 399–402.
- Maruta, H. & Korn, E. D. 1977b *J. biol. Chem.* **252**, 6501–6509.
- Maruta, H. & Korn, E. D. 1977c *J. biol. Chem.* **252**, 8329–8332.
- Mockrin, S. C. & Korn, E. D. 1980 *Biochemistry, Wash.* **19**, 5359–5362.
- Oosawa, F. & Asakura, S. 1975 *Thermodynamics of the polymerization of proteins*. New York: Academic Press.
- Pardee, J. & Spudich, J. A. 1982 *J. Cell Biol.* **93**, 648–654.
- Pollard, T. D. 1981 *J. biol. Chem.* **256**, 7666–7670.
- Pollard, T. D. & Korn, E. D. 1973a *J. biol. Chem.* **248**, 4682–4690.
- Pollard, T. D. & Korn, E. D. 1973b *J. biol. Chem.* **248**, 4691–4697.
- Pollard, T. D. & Mooseker, M. S. 1981 *J. Cell Biol.* **88**, 654–659.
- Pollard, T. D., Shelton, E., Wehling, R. R. & Korn, E. D. 1970 *J. molec. Biol.* **50**, 91–97.
- Pollard, T. D., Stafford, W., III & Porter, M. E. 1978 *J. biol. Chem.* **253**, 4798–4808.
- Reichstein, E. & Korn, E. D. 1979 *J. biol. Chem.* **254**, 6174–6179.
- Rich, S. A. & Estes, J. E. 1976 *J. molec. Biol.* **104**, 777–792.
- Rouayrenc, J. F. & Travers, F. 1981 *Eur. J. Biochem.* **116**, 73–77.
- Suck, D., Kabsch, W. & Mannherz, H. G. 1981 *Proc. natn. Acad. Sci. U.S.A.* **78**, 4319–4323.
- Tobacmann, L. & Korn, E. D. 1982 *J. biol. Chem.* **257**, 4166–4170.
- Tseng, P. & Pollard, T. D. 1982 *J. Cell Biol.* **94**, 213–218.
- Wakabayashi, T., Huxley, H. E., Amos, L. A. & Klug, A. 1975 *J. molec. Biol.* **93**, 477–497.
- Wehling, R. R. & Korn, E. D. 1971 *Biochemistry, Wash.* **10**, 590–600.
- Weisman, R. A. & Korn, E. D. 1967 *Biochemistry, Wash.* **6**, 485–497.

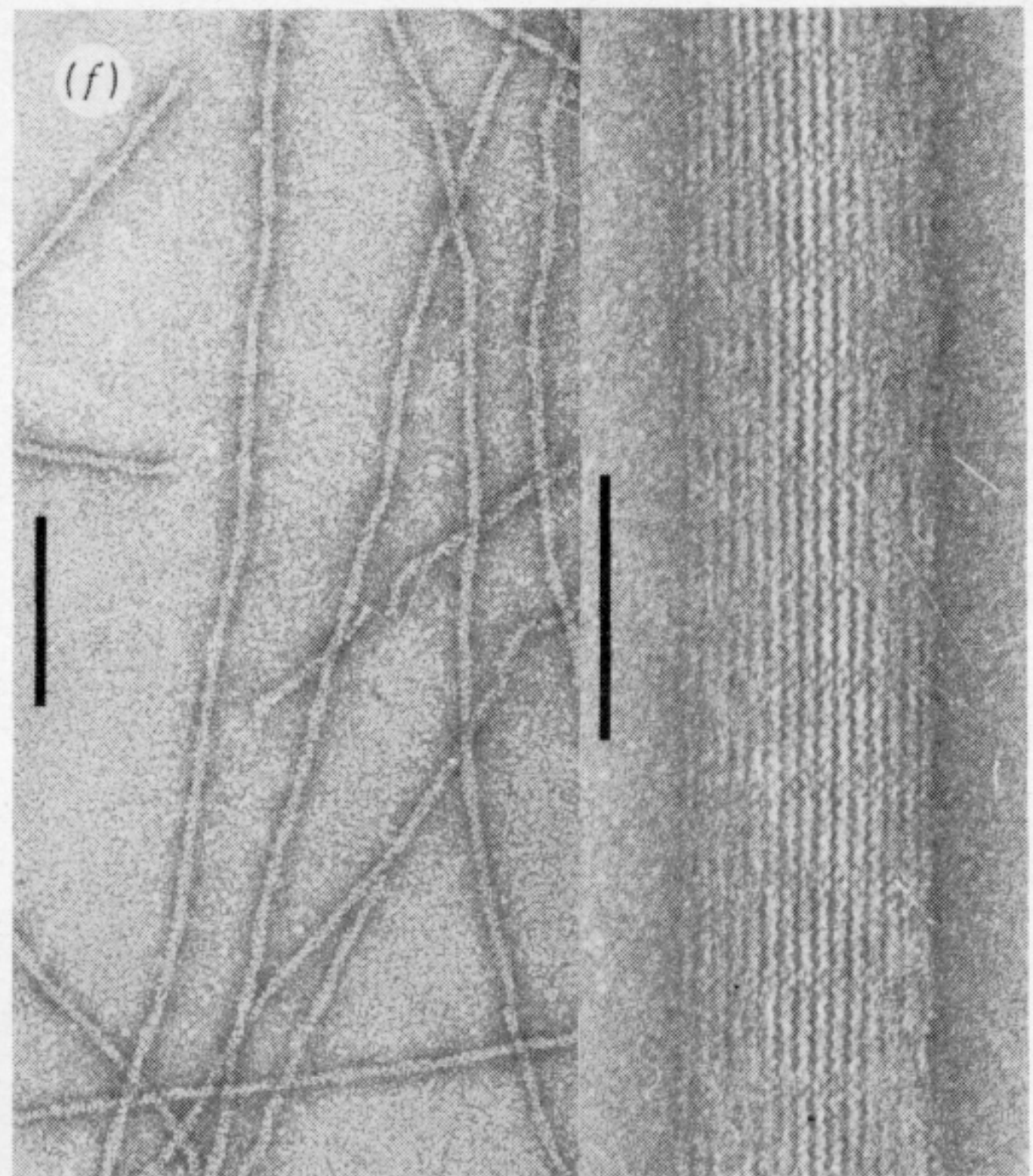
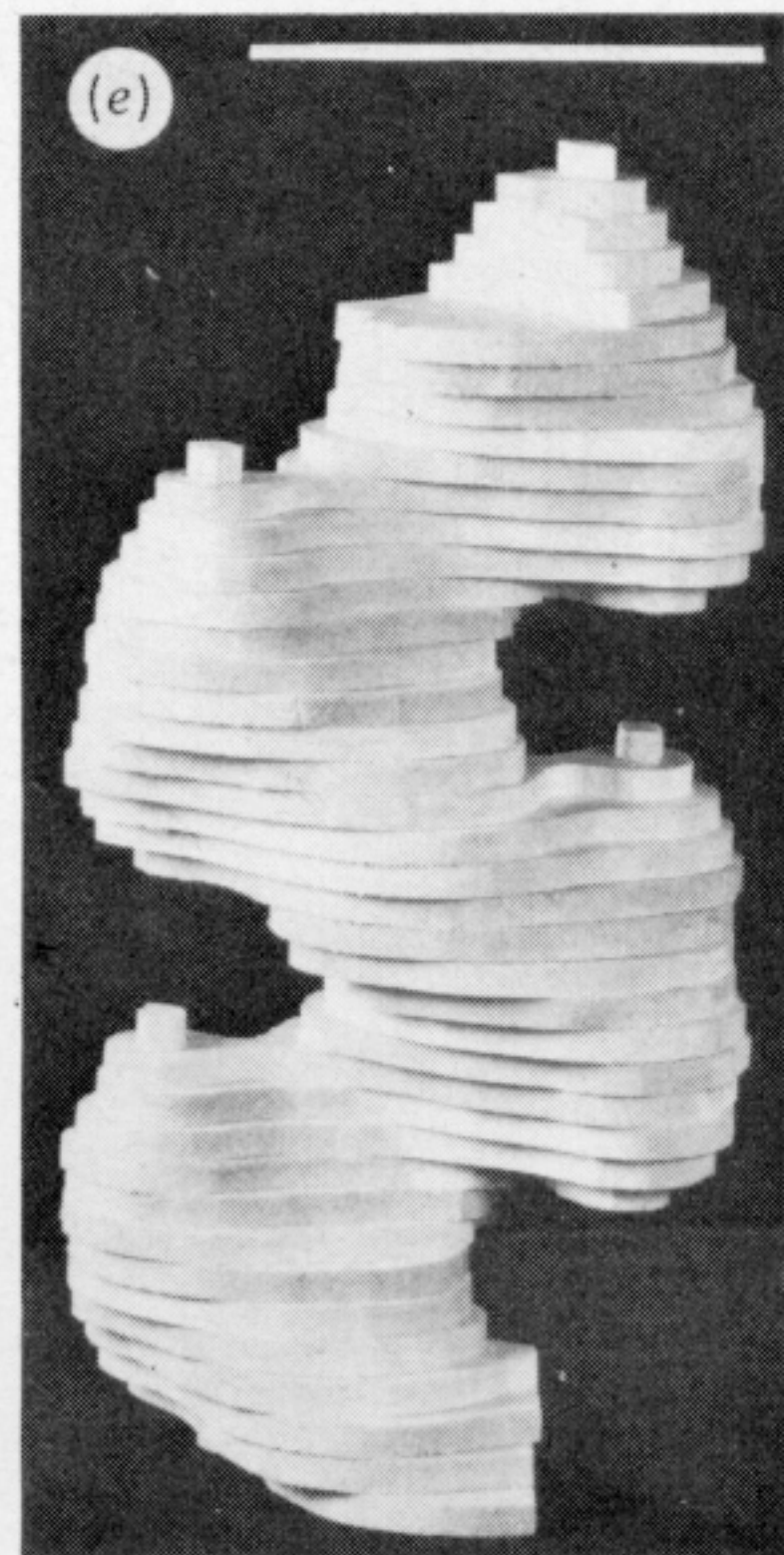
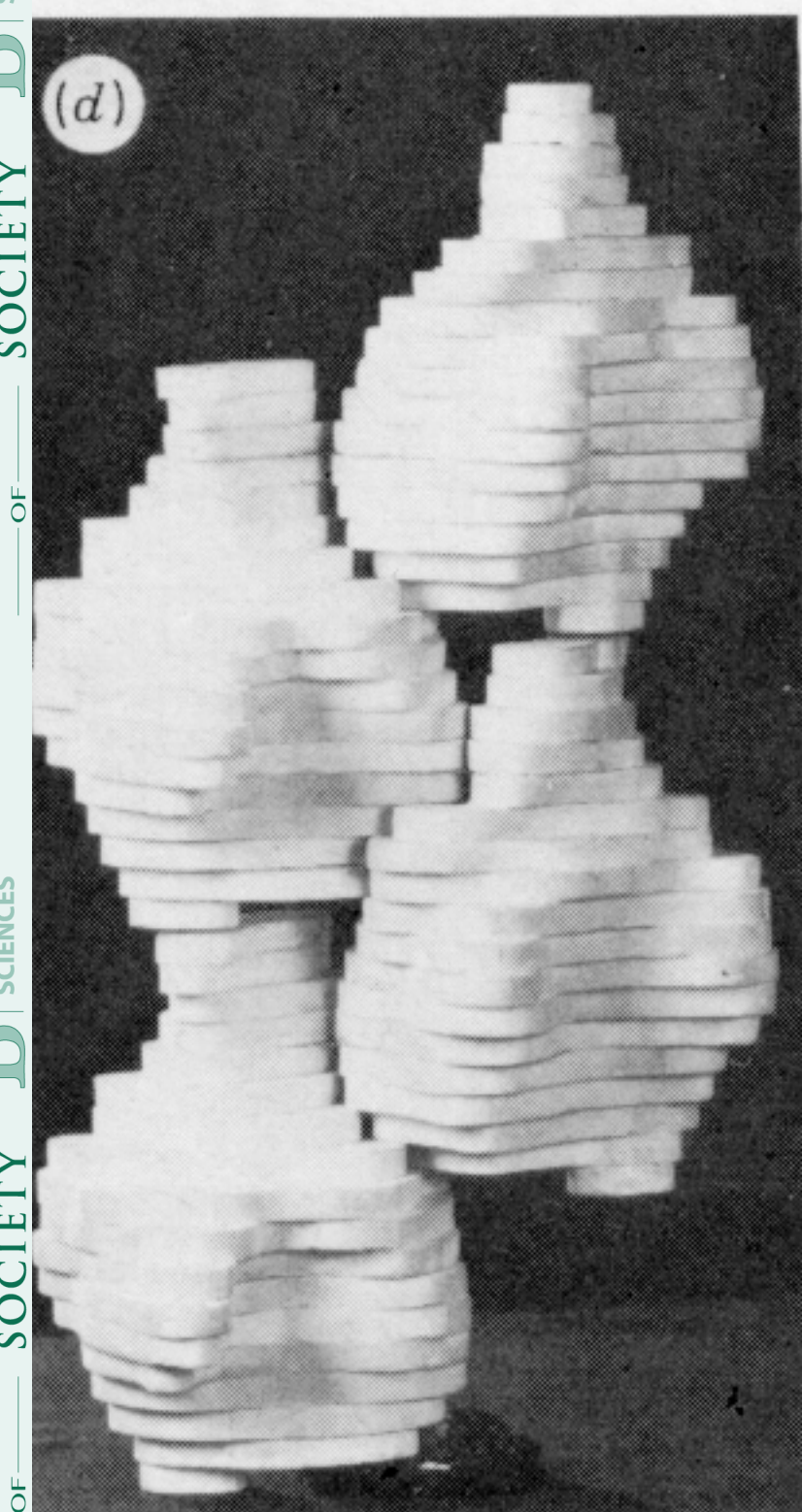
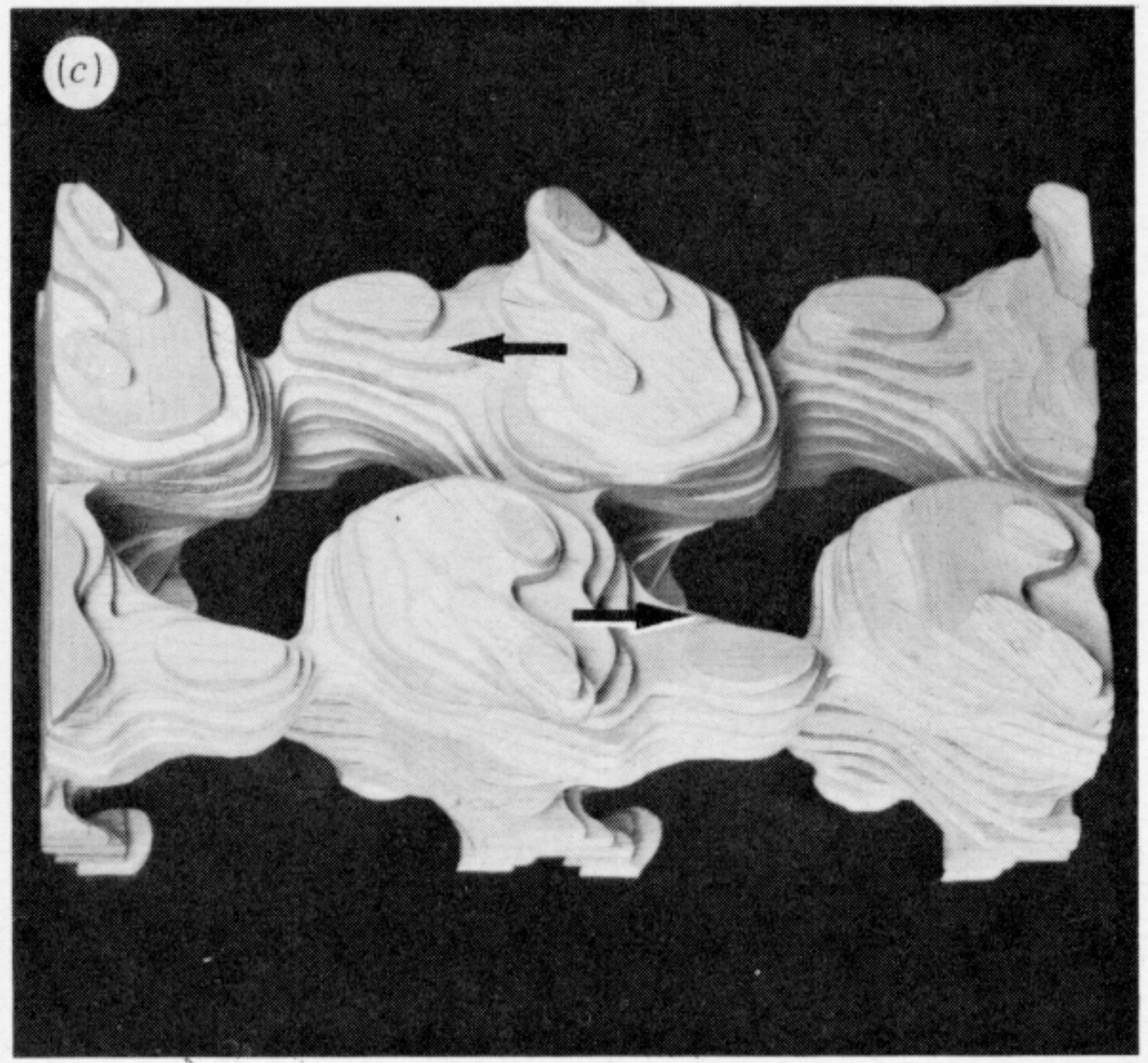
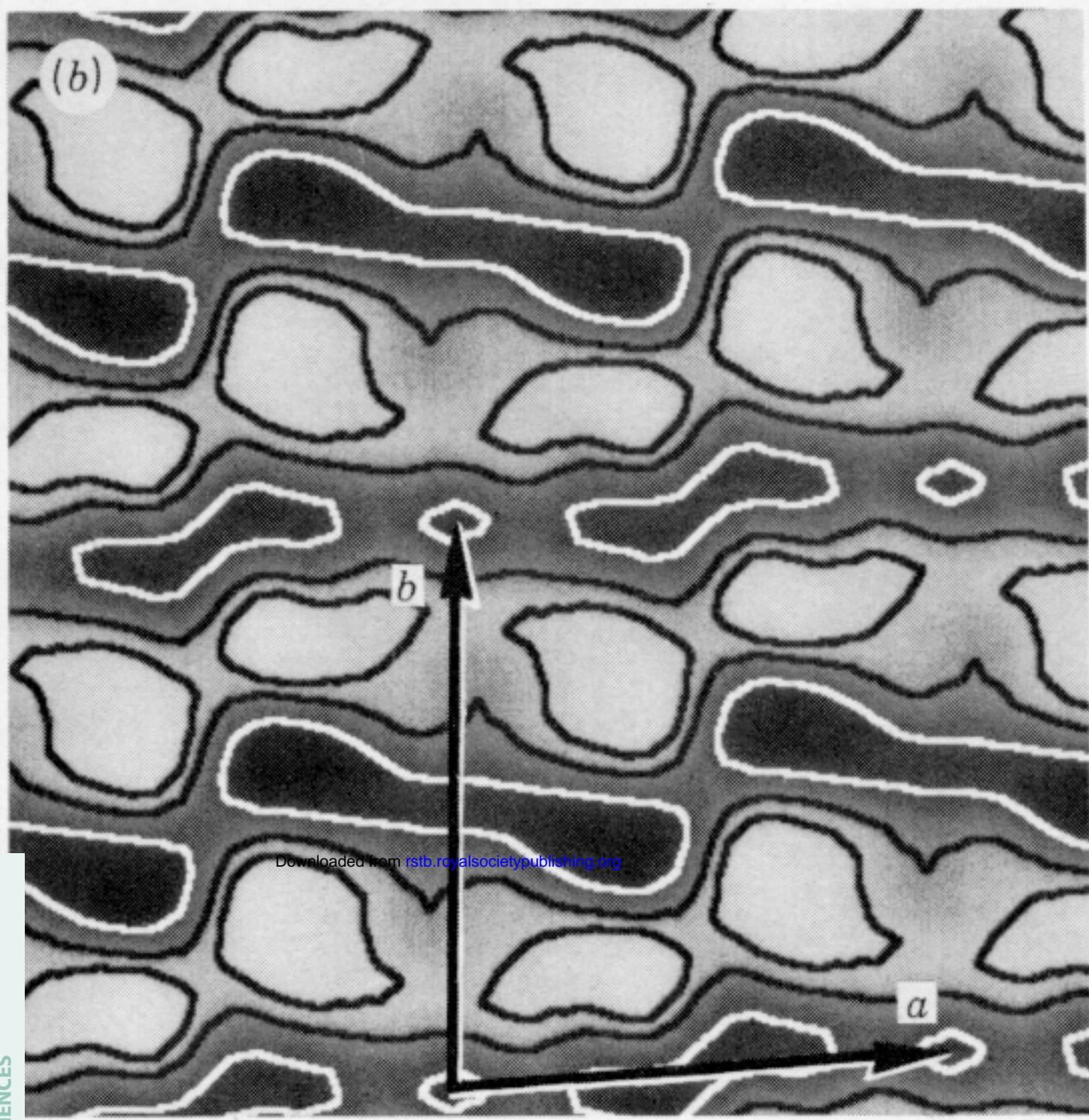
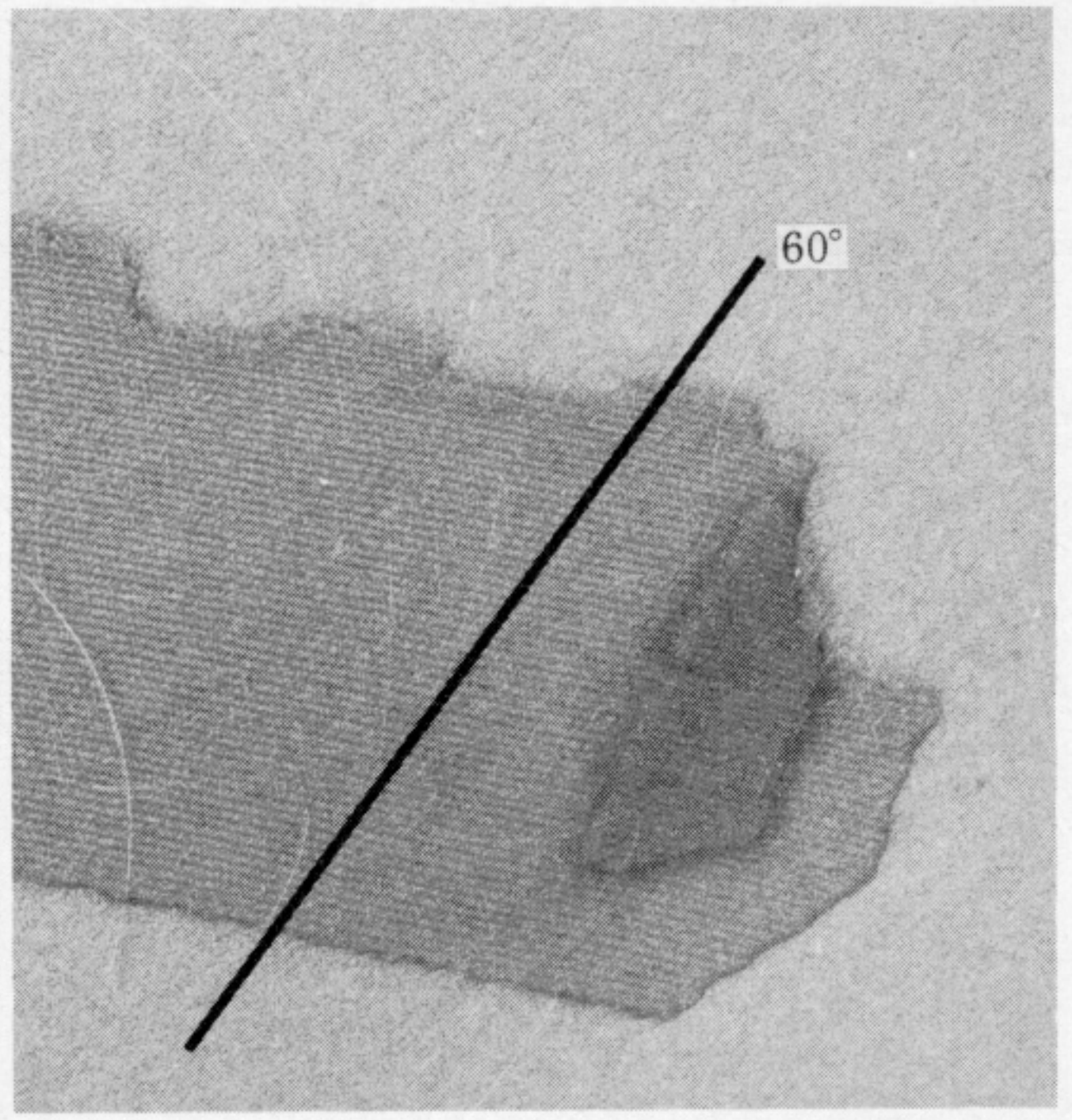
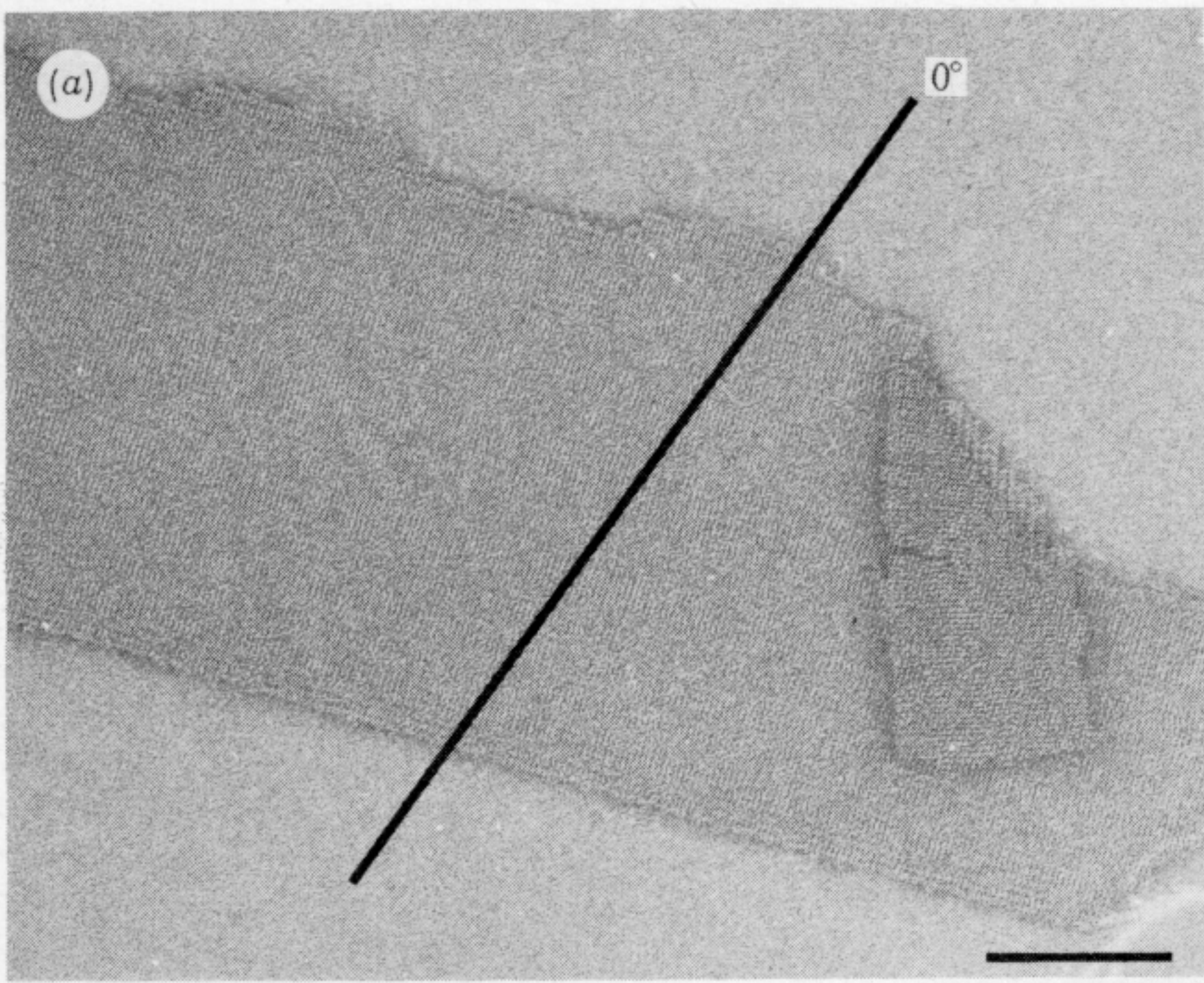


FIGURE 1. For description see opposite.

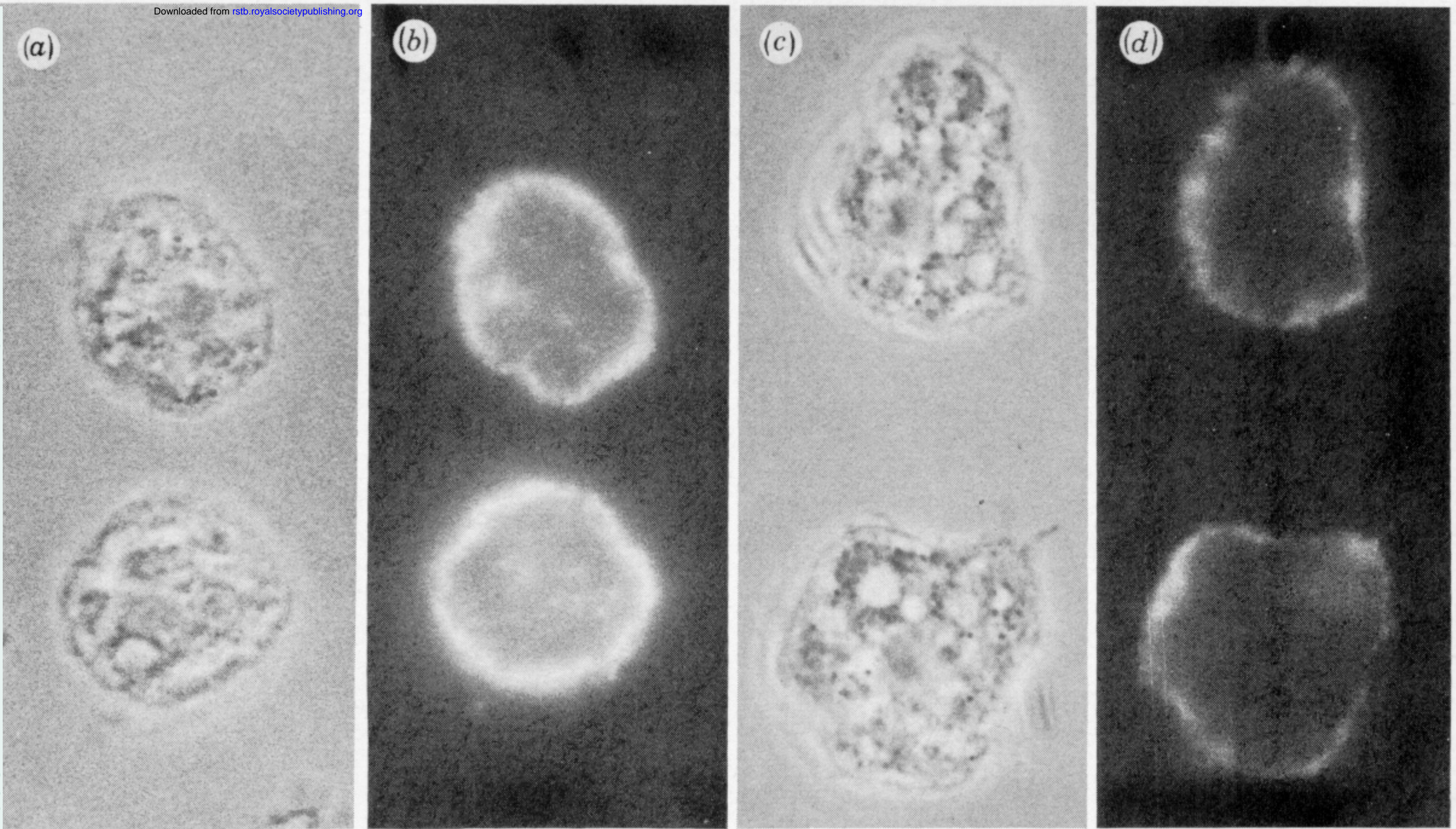


FIGURE 4. Localization in *Acanthamoeba* of actin filaments as shown with NBD-phalloidin (*a*, *b*) and capping protein with a purified antibody (*c*, *d*). Phase contrast (*a*, *c*) and fluorescence (*b*, *d*) micrographs of whole cells fixed with formaldehyde and permeabilized with acetone. (Work of J. A. Cooper.)

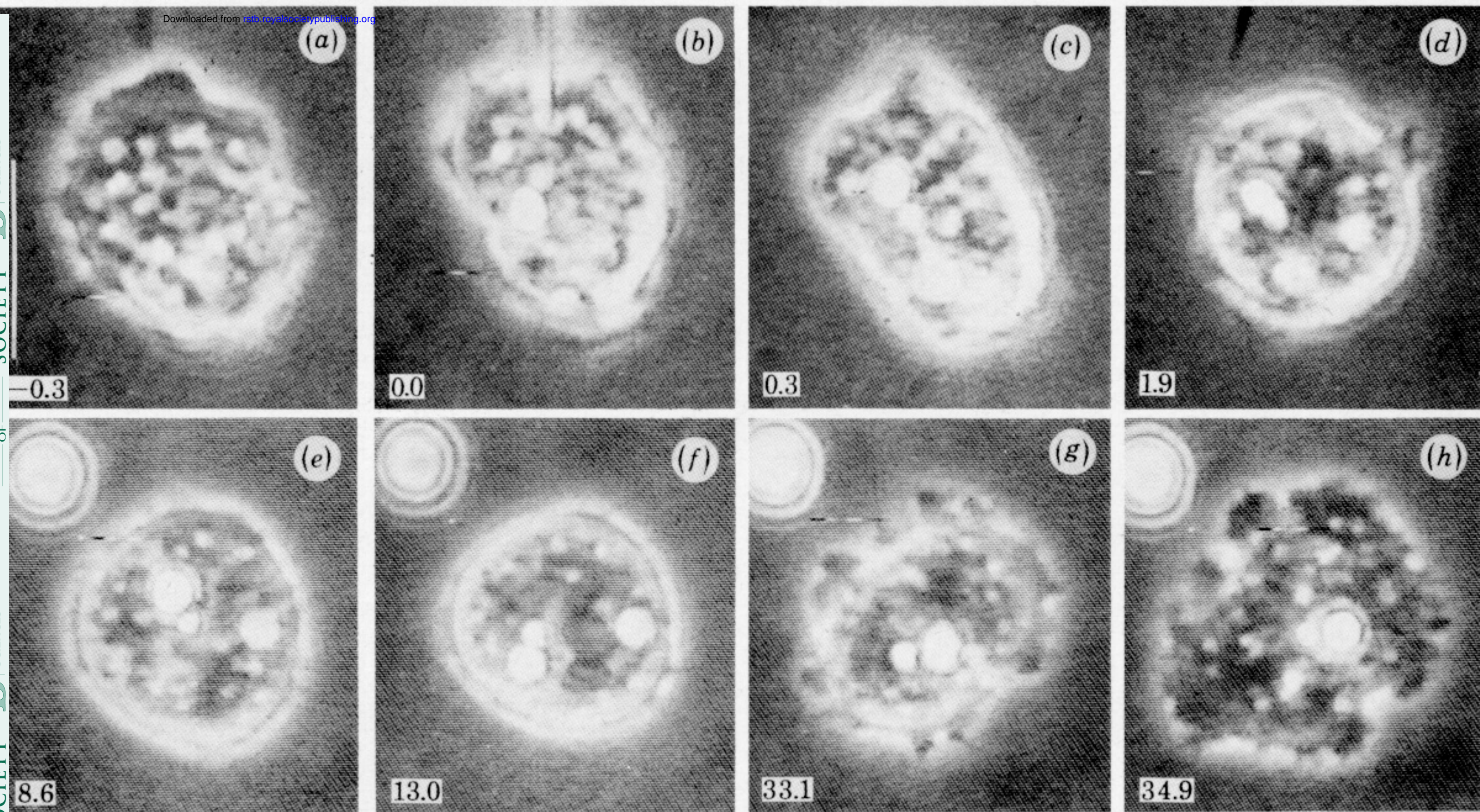


FIGURE 5. Microinjection of a living *Acanthamoeba* with 14 mg ml^{-1} monoclonal antibody MII.1 against myosin-II. This is a time sequence of phase contrast micrographs taken from (a) 0.3 min before microinjection to (h) 34.9 min afterwards. A droplet of oil equivalent in volume to the antibody injection ($2.6 \text{ pl} = 3.5\%$ of cell volume) is shown to the upper left of the cell in (e)–(h).